Environmental Science and Pollution Research (2023) 30:19259–19268
https://doi.org/10.1007/s11356-022-23546-z

RESEARCH ARTICLE

Chitosan cross-linked β–cyclodextrin polymeric adsorbent for the removal of perfluorobutanesulfonate from aqueous solution: adsorption kinetics, isotherm, and mechanism

Monu Verma[1,2] · **Ingyu Lee**[1] · **Vinod Kumar**[2,3] · **Shu-Yuan Pan**[4] · **Chihhao Fan**[4] · **Hyunook Kim**[1]

Received: 26 July 2022 / Accepted: 6 October 2022 / Published online: 13 October 2022
© The Author(s), under exclusive licence to Springer-Verlag GmbH Germany, part of Springer Nature 2022

Abstract

The existence of per- and polyfluoroalkyl substances (PFASs) in water is of serious interest due to their toxic, bioaccumulative, and persistent nature, and adsorption is an effective approach for the PFASs removal. In the present study, we developed a polymeric adsorbent by cross-linking chitosan and β–cyclodextrin using glutaraldehyde (Chi–Glu–β–CD) and evaluated its removal performance for perfluorobutanesulfonate (PFBS) from water. The results indicate that the performance was highly affected by solution pH; under a more acidic condition (e.g., pH 2.0), a higher removal efficiency was detected, and faster adsorption kinetics was observed with the rate constant (k_2) of $0.001 \pm 3\times10^{-4}$ g mg^{-1} min^{-1}. Adsorption isotherm data agreed to the Sips model with a maximum heterogeneous adsorption capacity of 135.70 ± 25.70 mg g^{-1}, probably due to protonated amine (NH^{+}) and electron-deficient β–CD cavities. The adsorption mechanism was confirmed using energy dispersive X-ray and Fourier transform infrared (FTIR) spectroscopy, showing the role of electrostatic attractions between the protonated amine and the negatively charged PFBS molecule (especially, with sulfonate side (N–H–-O–S)) and host–guest inclusion formations with β–CD cavity in adsorption. Additionally, the synthesized adsorbent was recovered using methanol without any significant decline in adsorption efficiency even after four continuous adsorption/desorption cycles. All these findings suggested that the Chi–Glu–β–CD composite could be a promising adsorbent in the removal of PFBS from water.

Keywords Cross-linked chitosan-β–cyclodextrin · PFBS removal · Kinetics and isotherms · Adsorption mechanism

Introduction

Per- and polyfluoroalkyl substances (PFASs) are man-made ubiquitous fluorinated organic chemicals which are extensively used at commercial and industrial levels as flame retardants in electronics fabrication facilities (fabs), corrosion inhibitors in aircraft hydraulic fluids, mist suppressants in the metal plating industry, aqueous film forming foams (AFFFs) products, and surfactants for enhanced recovery in oil production (Moody and Field 2000; Chen et al. 2020; Jacob et al. 2021). These chemicals are thermally and chemically stable due to their C–F bonds, which make them highly persistent in the environment (Houtz et al. 2013). A number of studies were reported on their adverse ecological and human health effects including bioaccumulation, cancer, immunotoxicity, and developmental disorder (Rae et al. 2015; Pan et al. 2017; Garg et al. 2020; Jacob et al. 2021). Until now, more than 4700 PFASs have been introduced in the global market, and these are continuously growing due to continuous synthesis of new/alternative PFASs (OECD

Responsible Editor: Guilherme L. Dotto

Highlights

- Chi–Glu–β–CD were synthesized for PFASs removal.
- Sips isotherm model showed adsorption capacity of 135.70±25.70 mg g^{-1}.
- Faster adsorption kinetics with k_2 0.001±3×10^{-4} g mg^{-1} min^{-1} at acidic solution.
- EDX, elemental mapping, and FTIR explained adsorption mechanism.
- Excellent reusability with methanol for further reuse.

✉ Hyunook Kim
h_kim@uos.ac.kr

[1] Water-Energy Nexus Laboratory, Department of Environmental Engineering, University of Seoul, Seoul 02504, South Korea

[2] Department of Life Sciences, Graphic Era (Deemed to Be University), Dehradun, Uttarakhand 248002, India

[3] Peoples' Friendship, University of Russia, RUDN University), Moscow 117198, Russian Federation

[4] Department of Bioenvironmental, Systems Engineering, National Taiwan University, Taipei 10617, Taiwan

2018). However, due to analytical limitations, only selected groups of PFASs have been examined (Glüge et al. 2020). In a recent review, the concentrations of perfluorooctanoic acid (PFOA) and perfluorooctanesulfonic acid (PFOS) in the effluent wastewater were reported from 10–100 to 7-50 ng L^{-1}, respectively, while concentrations of both pollutants reached up to 1 μg L^{-1} in some extreme cases (Trojanowicz et al. 2018).

Adsorption approach is one of the most successful and practical technique for the treatment of different types of PFASs owing to its higher removal efficiency, lower cost, and environment-friendly (e.g., byproduct-free) properties (Park et al. 2020). Recently, different types of adsorbents were employed in the PFASs removal such as metal organic frameworks, granular activated carbon (GAC), and other carbon materials, polymer materials, nanomaterials, etc. (Ochoa-Herrera and Sierra-Alvarez 2008; Sini et al. 2018; Vu and Wu 2020; Lenka et al. 2021). More recently, Wan et al. stated the use of coal combustion residuals-fly ash modified (FA-SCA) composite as an adsorbent in the rapid removal of PFOA and PFOS via the synergistic process of electrostatic and hydrophobic interactions (Wan et al. 2022). The study also showed that the removal efficiency could be maintained at ˃ 90% even after five continuous regeneration cycles. In another study, Choudhary et al. used an adsorbent prepared by cross linking β–cyclodextrin (β–CD) network with decafluorobiphenyl linkers to remove ammonium PFOA-based surfactant via electrostatic and hydrophobic interactions (Choudhary et al. 2022). In these interactions, the β–CD segments facilitate the attraction of anionic headgroup of PFOA, while fluorinated linkers offer an additional hydrophobic attraction for the PFOA tail as well as higher affinity of the network toward PFOA in comparison with hydrocarbons. Until now, GAC is considered as an effective and affordable adsorbent. However, it has some shortcomings such as low adsorption capacity for PFAS molecules which makes it ineffective in adsorbing the molecules at environmental levels. It also requires higher energy input in the process of its regeneration process (Eschauzier et al. 2012). Therefore, it is urgently needed to develop other adsorbents that can effectively overcome the shortcomings.

Chitosan (Chi) is a well-known linear chain polyaminosaccharide, obtained from chitin via alkaline deacetylation process, and widely used in the removal of water contaminants (e.g., PFASs) due to various valuable structural and functional properties. Chi has the merits of low toxicity, biodegradability, biocompatibility, and good miscibility with other polymers. It has also a highly chemically reactive structure due to the presence of primary amines (Zargar et al. 2015). β-cyclodextrin is another important macrocyclic molecule comprised of seven glucose units and attracts great attentions due to aromatic pollutants encapsulation selectively through well-defined host–guest complexation effect (a hydrophilic outer edge and inner hydrophobic inner cavity structure) (Alsbaiee et al. 2016). Few authors have reported the application of the composites of Chi and β–CD in the wastewater treatment to remove both organic and inorganic pollutants (Zhao and Sillanpää 2020).

In this research work, a versatile adsorbent was prepared using Chi and β–CD polymers with glutaraldehyde (Glu) as a cross-linker and investigated to evaluate the adsorption performance for perfluorobutanesulfonic acid (PFBS; a well-known compound of PFASs group) in water. Different batch experiments were performed to further evaluate the optimum adsorption efficiency of the synthesized Chi–Glu–β–CD adsorbent by varying the solution pH, contact time, and initial PFBS concentrations. The used adsorbents were also reused after regeneration. To the best of our knowledge, no one has reported the synthesis of Chi–Glu–β–CD polymeric adsorbent and batch parameters for the adsorptive removal of PFASs pollutants from aqueous solution.

Materials and methods

Chemicals

The chemicals of analytical or HPLC grade were used during all the experiments. Deacetylated chitosan flakes (+85%) and β–cyclodextrin (˃ 97%) were purchased from Sigma-Aldrich (Seoul, Korea); the viscosity and MW (molecular weight) of the polymers were 200–2000 MPa s and 190,000–375,000 g mol^{-1}, respectively. Glutaraldehyde (50%, w/v) was purchased from Junsei (Kyoto, Japan). Perfluorobutanesulfonic acid (> 97% purity) was purchased from Sigma-Aldrich (Seoul, Korea). Deionized water (DI) was used for all experiments.

Chi–Glu–β–CD preparation

Chi–Glu–β–CD composite was synthesized by modifying the reported procedure (Wilson et al. 2013; Verma et al. 2021). Briefly, 1.0 g Chi and 6.0 g β–CD were dissolved overnight in 100 mL of 0.002 M acetic acid in a 300-mL round bottom flask at 50 °C. Then, 3.0 mL Glu was added rapidly to the mixture to induce rapid gelation within ~ 1 min. During this reaction, transparent solution became yellow orange (dark) within 60 min. The mixture was left for 2 h for complete gelation before neutralizing with 0.2 M NaOH. Thereafter, the product was washed several times with cold DI water and cold acetone, followed by being dried overnight at 55 °C in a vacuum oven. The dried product was ground into fine powder and then washed with methanol three times followed by washing with diethyl ether. The schematic presentation of the Chi–Glu–β–CD product is shown in Scheme 1.

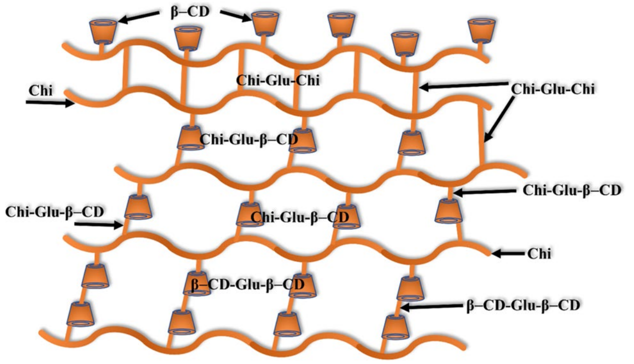

Scheme 1 A framework structure of the synthesized Chi–Glu–β–CD polymeric structure

Characterizations

A field emission scanning electron microscopy (FESEM, SU8010, Hitachi, Tokyo, Japan) was used to observe the surface structure of the synthesized Chi–Glu–β–CD adsorbent, and the structural analysis was further carried out by a powder X-ray diffractometer (AXS D8 Advance, Bruker, Billerica, MA, USA) equipped with a Cu K_α radiation source ($\lambda = 0.154$ nm). Elemental mapping and compositional analysis were performed during FESEM analysis using the Thermo Scientific Ultra Dry Energy Dispersive X-ray spectroscopy (EDS) detector. Fourier transform infrared spectroscopy (FTIR, Nexus 670, Thermo Electron, Waltham, MA, USA) was used to check the functional groups available on the adsorbent. Thermal stability was recorded on thermogravimetry analyzer (TGA, EXSTAR 6300, Seiko Instrument, Chiba, Japan) in the range 25–800 °C with the heating rate of 10 °C min^{-1}. Initial and final concentration of the used PFBS was quantified using LCMS (LCMS-8050, Shimadzu, Kyoto, Japan) through the multiple reaction monitoring (MRM).

Batch adsorption

200 mg L^{-1} standard solution of PFBS was prepared for all batch experiments, and all the adsorption experiments were conducted with the 10 mL of the prepared pollutant with 12 mg of adsorbent dose at a stirring speed of 150 rpm. pH effect was conducted in the range of 2.0-10.0 with the solution containing PFBS at the initial concentration of 50 mg L^{-1}. pH was adjusted with 0.1 M HCl and 0.1 M NaOH. Adsorption isotherm experiments were performed with PFBS in the range of 1-160 mg L^{-1}, while kinetics experiments were conducted in the time range of 1-360 min.

Then, filter the mixture with 0.45-μm filter to separate out the liquid and adsorbent. For regeneration, 12 mg adsorbent was added to 50-mg L^{-1} PFBS of 20 mL at pH 4.0. After the mixture was shaken for 300 min, the material was separated through centrifugation and then washed with 30-mL methanol (Alsbaiee et al. 2016). Thereafter, this regenerated adsorbent was dried in a vacuum oven to avoid the methanol effect on PFBS adsorption. This reuse test was performed four times continuously under the same conditions. For kinetics and isotherms studies, the initial concentration of 50 mg L^{-1} was used. During the experiments for evaluating pH effect, concentration effect, and regeneration efficiency, contact time of 480 min was chosen for complete equilibrium. The % removal and adsorption capacity (g mg^{-1}) of PFBS on the Chi–Glu–β–CD adsorbent were calculated according to previously reported mathematical formulas (Verma et al. 2022c).

Mathematical modeling

Three models for adsorption kinetics, i.e., pseudo-first order (PFO), pseudo-second order (PSO), and Elovich models, were used which are presented as follows, respectively.

$$q_t = q_e(1 - e^{-k_1 t}) \tag{1}$$

$$q_t = \frac{k_2 q_e^2 t}{1 + k_2 q_e t} \tag{2}$$

$$q_t = \frac{1}{\beta} ln(\alpha \beta t) \tag{3}$$

where q_t and q_e represent the adsorbed amount of PFBS in milligram gram^{-1} at time t (min) and at equilibrium, respectively. k_1 (min^{-1}) and k_2 (g mg^{-1} min^{-1}) are the rate constants for PFO and PSO models, respectively. α is the initial adsorption rate (mg g^{-1} min^{-1}), and β is the desorption constant (g mg^{-1}).

The isotherm data were investigated using three isotherm models: Langmuir, Freundlich, and Sips models which are presented by the following equations, respectively.

$$q_e = \frac{q_m K_L C_e}{1 + K_L C_e} \tag{4}$$

$$q_e = K_F C_e^{1/n} \tag{5}$$

$$q_e = \frac{q_m \left(K_S C_e\right)^{1/n_s}}{1 + \left(K_S C_e\right)^{1/n_s}} \tag{6}$$

where C_e (mg L^{-1}) and q_e (mg g^{-1}) indicate the PFBS concentration in water and adsorption capacity at equilibrium, respectively. K_L and q_m (mg g^{-1}) indicate the adsorption energy-related Langmuir constant and the maximum adsorption capacity of Chi–Glu–β–CD, respectively. n and K_F represent the Freundlich constants associated with the heterogeneity and adsorption intensity of adsorbent, respectively. n_s and K_s are the Sips constants related to energy constants and heterogeneity factor, respectively. All these values are obtained from nonlinear fitting of experimental data.

The kinetic and isotherm parameters were calculated using nonlinear regression (Origin Version 22b). Chi-square (χ^2) test was used to evaluate the best fitting data (Eq. 7).

$$\chi^2 = \sum \frac{(q_{\mathrm{exp}} - q_{\mathrm{cal}})^2}{q_{\mathrm{cal}}} \tag{7}$$

where q_{exp} and q_{cal} are experimental and model-calculated values of adsorption capacity (mg g^{-1}), respectively.

Results and discussion

Structural characteristics

The surface morphology of the prepared Chi–Glu–β–CD adsorbent is shown in Fig. 1a, indicating polymer-like sheet structure with some porosity due to cross-linking copolymerization between Chi and Glu. This structure provides more active sites for the adsorption of PFBS. FTIR spectroscopy was firstly used to identify the available functional groups on the prepared Chi—Glu–β–CD adsorbent (Fig. 1b). The characteristics peaks were found at 3353 cm^{-1} (stretching vibrational bands of O–H and N–H), 2932 and 2874 cm^{-1} (stretching vibrational bands of C–H), 1648 cm^{-1} (bending vibrational band of the N–H), 1384 cm^{-1} (bending vibrational band of the O–H group), and 1037 cm^{-1} (antisymmetric vibrational band of the C–O–C). Apart from them, two new peaks were noticed at 1557 (C–C) and 1658 (H–N) cm^{-1} which confirmed the formation of Chi–Glu–β–CD by the cross-linking between the amine group of Chi and the aldehyde group of Glu (Fan et al. 2013; Verma et al. 2021). Previously, Wilson et al. (2013) reported the cross-linking between the Chi and Glu via glyoxal intermediate. The frequency observed at 1658 cm^{-1} is due to the imine (C = N) formation between the amine group of Chi and the aldehyde group of Glu. In addition, aldol condensation seemed to happen between the –OH group of β–CD and –CHO group of Glu, which was confirmed by the variation frequency of C–O and –OH observed in the 1000–1200 cm^{-1} and ~ 3400 cm^{-1} frequency regions, respectively (Wilson et al. 2013). The powder XRD pattern of the prepared adsorbent shown in Fig. 1c also confirms the cross-linking reaction in the formation of amorphous structure by showing a broad peak at 19.4° instead of multiple peaks of β–CD and two peaks of Chi (Verma et al. 2022c). As shown in Fig. 1d, the TGA curve is indicating three thermal events in the range of 25–110 °C, 190–350 °C, and 350–600 °C. These thermal ranges show the weight loss of 13.4%, 37.2%, and 46.1% due to desorption of water, decomposition of binary Chi–Glu and β–CD–Glu copolymer, and decomposition of Chi and β–CD in Chi–Glu–β–CD composite, respectively (Wilson

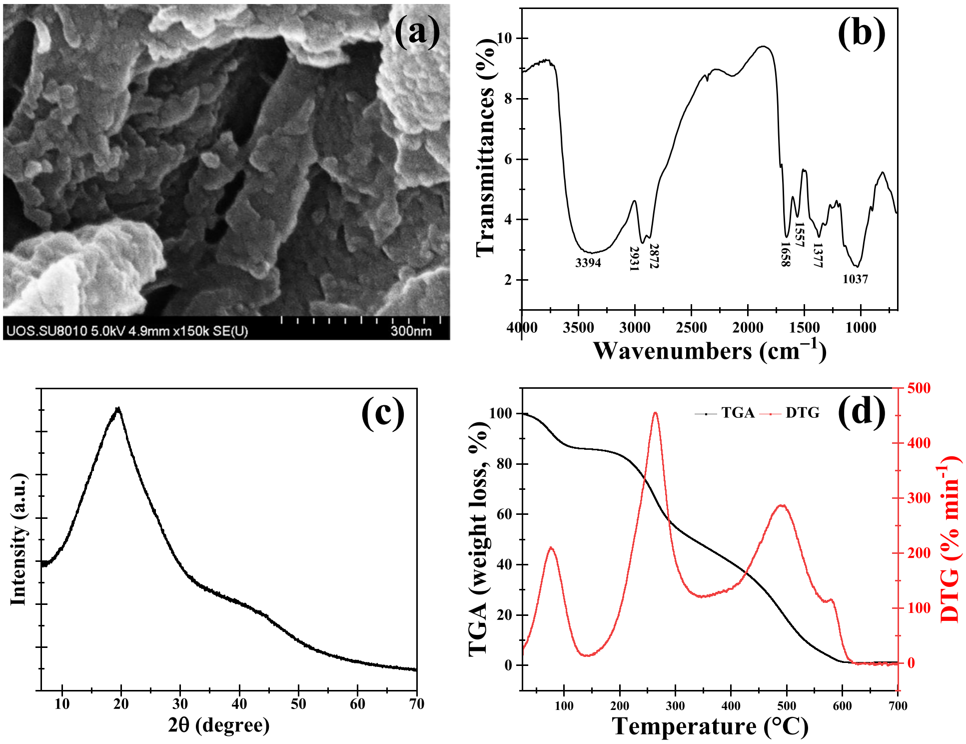

Fig. 1 **a** FESEM image, **b** FTIR, **c** powder XRD, and **d** TGA and DTG of the Chi–Glu–β–CD adsorbent

et al. 2013). DTG curve clearly supports the TGA data by showing three pyrolysis steps, illustrated by three peaks at 76.5 °C, 262 °C, and 490 °C.

Effect of pH

Figure 2 shows the effect of pH on the adsorption of PFBS onto Chi–Glu–β–CD composite. Data indicates that the percentage removal of PFBS decreased from 92.9 to 11.30% with increasing pH from 2.0 to 10.0. This higher removal efficiency at low pHs was due to existence of anionic form of PFBS ($pK_a = -3.31$), while the surface functional groups of the adsorbent were protonated under acidic condition. Thus, when the solution pH was 2.0, the surface of Chi–Glu–β–CD adsorbent had highly positive charge (due to $\mathrm{pH_{PZC}} = 8.7$), implying the electrostatic attraction between the positively charged surface of the adsorbent and the negatively charged PFBS molecules. As the solution pH was increased from 2.0 to 8.0, the adsorbent surface became less charged. At pH 8.0 to 10.0, the surface became negatively charged, resulting in the decreased removal efficiency of PFBS due to electrostatic repulsion. It is interesting to note that, at pH 10.0, removal efficiency 11.30% was also observable still after the electrostatic repulsion. This may be probably due to the electron-deficient cavities of β–CD. These cavities were relatively hydrophilic to allow faster diffusion of water and PFBS molecules. These cavities could form host–guest inclusion complex with the PFBS molecules. Wang et al. (2021) also reported the adsorption of four perfluoroalkane sulfonates (PFSAs) molecules onto β–CD covalent organic frameworks (β–CD–COFs) through pores and hydrophobic interaction with the electron-deficient β–CD cavities. Therefore, for further experiments, we chose pH 4.0 due to the acidic nature of wastewaters (Deng et al. 2010; Wang et al. 2021).

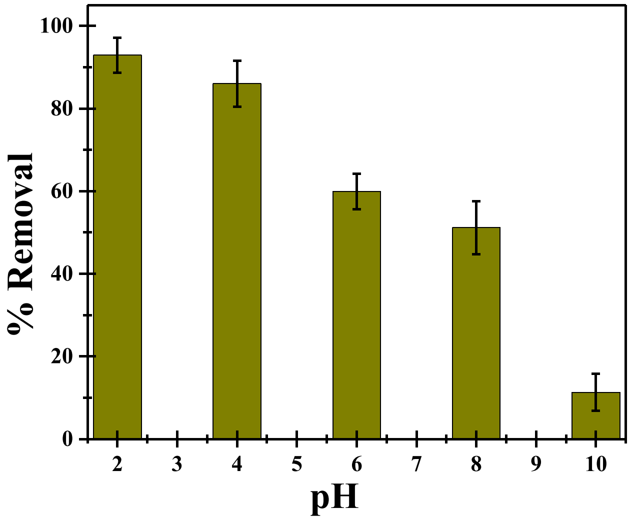

Fig. 2 Effect of pH on the removal efficiency of PFBS onto Chi–Glu–β–CD adsorbent

Effect of contact time and adsorption kinetics

The effect of contact time on the adsorption efficiency of PFBS onto Chi–Glu–β–CD adsorbent was investigated to know how long it takes to arrive at equilibrium (Fig. 3a). The figure indicates the faster adsorption in the initial period of the contact time (i.e., up to 30–60 min) and then arrival at the equilibrium after 200 min. This faster adsorption was probably due to the availability of active sites and β–CD's cavities which became saturated with time and arrived at the equilibrium in the later stage of the reaction. The removal efficiency was ~ 75% in the starting stage of 60 min and reached up to ~ 96% at equilibrium.

The experimental kinetics data was fitted to PFO, PSO, and Elovich models (Fig. 3b), and the fitting results are listed in Table 1. The data better fitted to the PSO kinetics model; higher R^2 (= 0.984) and lesser χ^2 (= 0.632) was observed, comparing to the values obtained with the PFO and Elovich models which corresponded to 0.940/0.916 and 1.484/2.536, respectively. Also, the adsorption capacity ($q_{e,\mathrm{cal}} = 39.75 \pm 1.30$) calculated with the PSO was close to the experimental adsorption capacity ($q_{e,\mathrm{exp}} = 39.60 \pm 2.50$), again confirming the better fit with the PSO kinetics model. Similar type of adsorption kinetics results were reported previously (Son and An 2022).

Effect of initial concentration and adsorption isotherms

The adsorption isotherm of PFBS onto Chi–Glu–β–CD adsorbent was investigated to know the effect of initial concentration on the removal efficiency, and results are shown in Fig. 3c. Based on data, higher removal efficiency could be observed at lower concentrations. However, the efficiency decreased continuously with the initial concentration increasing, which was possibly due to availability of abundant adsorption sites. As the initial concentration of adsorbate increased, adsorption sites gradually decreased, which led to loss in removal efficiency. The isotherm data also indicated almost vertical curve which indicates a good affinity of PFBS towards the synthesized adsorbent. It is also interesting to note that adsorption capacity of the adsorbent increased almost linearly with the initial concentration of PFBS (Fig. 3d). This was possibly due to more pores and functional groups on the adsorbent that could accommodate more PFBS molecules.

Three isotherm models, i.e., Langmuir, Freundlich, and Sips (Verma et al. 2022a, b), were applied to fit the isotherms data to quantitatively evaluate the adsorption capacity of the synthesized composite (Fig. 3d), and their

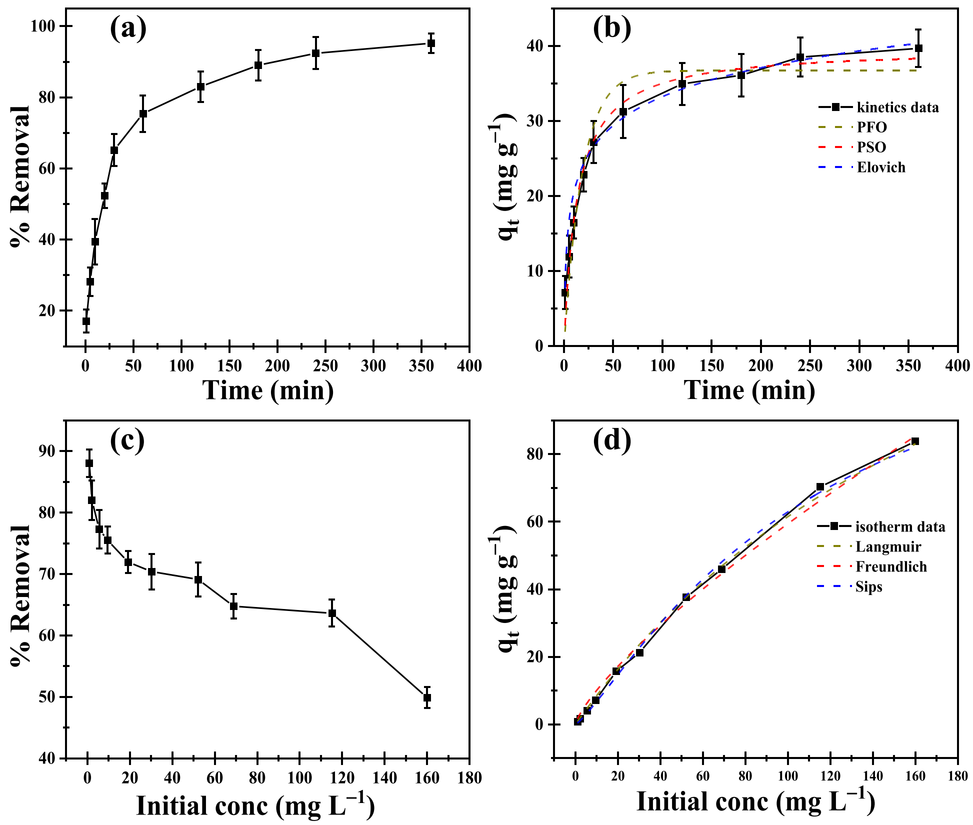

Fig. 3 **a** Contact time effect on removal efficiency, **b** nonlinear kinetics isotherms, **c** effect of initial concentration on adsorption efficiency, and **d** nonlinear adsorption isotherm for PFBS adsorption onto Chi–Glu–β–CD adsorbent

Table 1 Fits of PFO, PSO, and Elovich kinetics models to adsorption of PFBS onto Chi–Glu–β–CD adsorbent

Models	Parameters	PFBS
PFO	$q_{e,\mathrm{exp}}$ (mg g^{-1})	39.60 ± 2.50
	$q_{e,\mathrm{cal}}$ (mg g^{-1})	36.70 ± 1.55
	k_1 (min^{-1})	0.053 ± 0.002
	R^2	0.940
	χ^2	1.484
PSO	$q_{e,\mathrm{cal}}$ (mg g^{-1})	39.75 ± 1.30
	k_2 (g mg^{-1} min^{-1})	0.001 ± 3×10^{-4}
	R^2	0.984
	χ^2	0.632
Elovich	α (mg g^{-1} min^{-1})	22.30 ± 1.10
	β (g mg^{-1})	0.180 ± 0.001
	R^2	0.916
	χ^2	2.536

Table 2 Fitting result of three isotherm models to adsorption of PFBS onto Chi–Glu–β–CD adsorbent

Models	Parameters	PFBS
Langmuir	$q_{m,\mathrm{exp}}$ (mg g^{-1})	79.80 ± 4.45
	$q_{m,\mathrm{cal}}$ (mg g^{-1})	199.35 ± 27.70
	k_1 (min^{-1})	0.004 ± 9.1×10^{-4}
	R^2	0.933
	χ^2	6.283
Freundlich	K_F (mg g^{-1})	1.70 ± 0.412
	n	1.30 ± 0.08
	R^2	0.986
	χ^2	13.282
Sips	$q_{m,\mathrm{cal}}$ (mg g^{-1})	135.70 ± 25.70
	K_S L (mg^{-1})	0.008 ± 0.002
	n_s	0.995
	χ^2	5.301

corresponding calculated parameters are listed in Table 2. As a result, the Langmuir and Sips models were well fitted to the experimental data; the obtained R^2 values were 0.993 and 0.995, respectively, while the one for Freundlich model was 0.986. However, the closer the calculated adsorption capacity ($q_{m,\mathrm{cal}}$) with the experimental adsorption capacity (q_{m},$_{\mathrm{exp}}$) and the lesser the χ^2 value for the Sips model strongly illustrates that a better fit was obtained with the Sips model instead of the Langmuir and Freundlich models (Badruddoza et al. 2017; Wang et al. 2021). The Freundlich isotherm indicator n value for PFBS adsorption was 1.30, indicating nonlinear adsorption and some interactions such as host–guest inclusion complex might be involved (Wang et al. 2021).

Adsorption mechanism

Based on the experimental results, the mechanism for the adsorption of PFBS onto the Chi–Glu– β–CD adsorbent can be explained by the role of electrostatic attraction and the host–guest inclusion complex formation (hydrophobic interaction). The EDS spectrum for the adsorbent obtained after the adsorption of PFBS indicates the uniform distribution and higher content (5.66%) of *F* (*F* indicates PFBS), confirming the adsorption of PFBS uniformly onto the surface of adsorbent (Fig. 4).

The FTIR spectrum (Fig. 5a) confirmed the adsorption mechanism by showing that the peaks were almost similar to the raw adsorbent; the intensity of only few peaks was depressed due to electrostatic attraction and host–guest inclusion complex formation. PFBS has the structure with sulfonate head and C–F chain tail, while β–CD consists of a regular cavity with proper size and structure, resulting in tight adsorption of PFBS molecules. In the acidic solution, the adsorbent possesses electron-deficient protonated amine groups which show strong electrostatic interactions with highly negatively charged PFBS molecules, especially with the sulfonate side (N–H--O–S) and C–F. Previously, it was reported that the cavities of β–CD would be relatively electron-deficient while outer part be electron-rich (Crini 2014). As PFBS molecule is highly electron-rich, therefore, β–CD have the tendency to capture PFBS in the cavity in a complement manner. Previously, Wang et al. (2021) studied the adsorption of different types of PFAS molecules onto the cyclodextrin covalent organic frameworks through the hydrogen bonding between the sulfonated head of PFAS and amino groups, and the inclusion into the cavity of β–CD. They also reported the van der Waals interaction between the C–F of PFAS and ether ring of β–CD. Scheme 2 represents the adsorption mechanism of the PFBS onto Chi–Glu–β–CD adsorbent.

Fig. 4 **a** EDS mapping of Chi–Glu–β–CD adsorbent; FESEM image with elements highlighting the region used for EDS analysis, **b** N Ka1 mapping, **c** C Ka1 mapping, **d** O Ka1 mapping, **e** F Ka1 mapping, and **f** EDS spectra and elemental composition of the composite surface

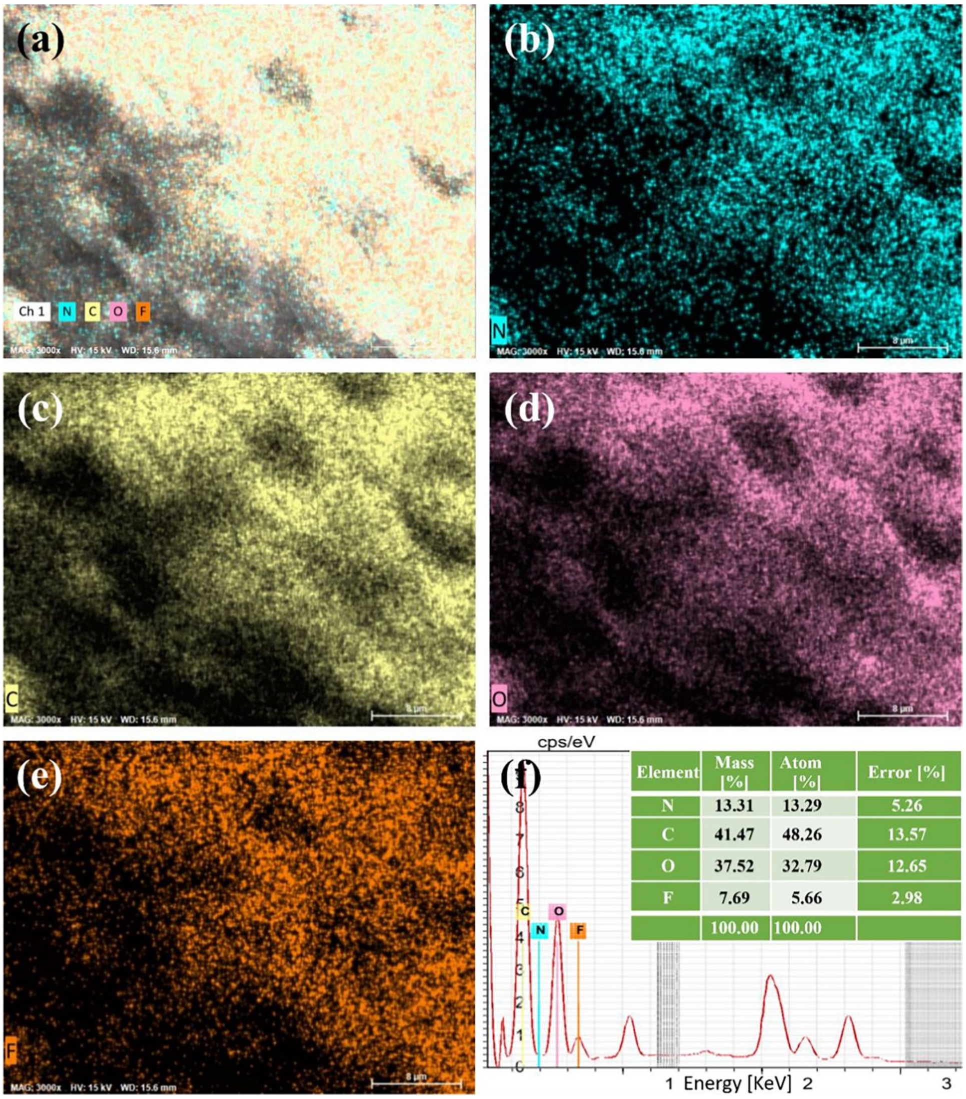

Element	Mass [%]	Atom [%]	Error [%]
N	13.31	13.29	5.26
C	41.47	48.26	13.57
O	37.52	32.79	12.65
F	7.69	5.66	2.98
	100.00	100.00	

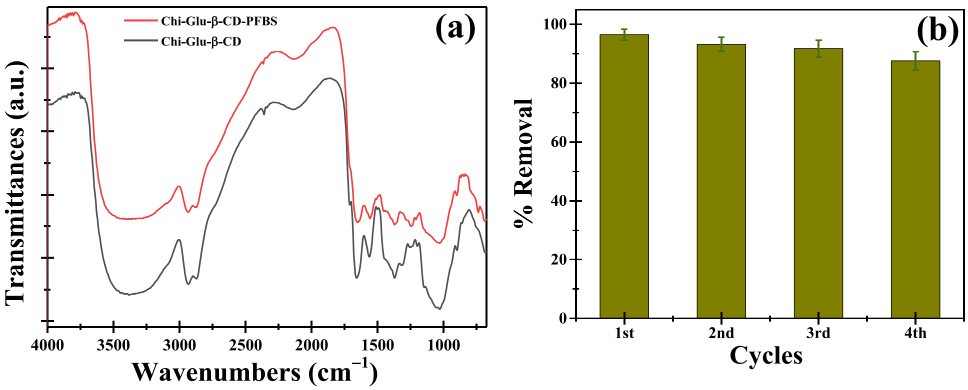

Fig. 5 **a** FTIR spectra before and after PFBS adsorption and **b** regeneration efficiency in four continuous cycles

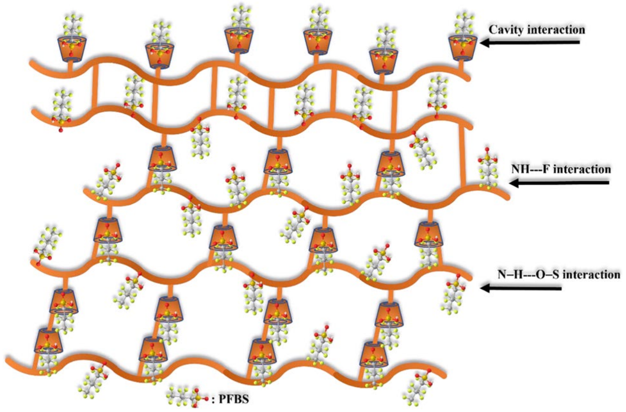

Scheme 2 Adsorption mechanism of PFBS on Chi–Glu–β–CD adsorbent

Regeneration and reusability

To regenerate the spent adsorbents, different types of strategies such as organic solvent, hot water, advanced oxidation, and ultrasonication have been used (Wang et al. 2019). Among them, a better desorption efficiency without material loss could be observed by using solvent. Ethanol and methanol solvents were previously reported to regenerate the activated carbon and β–CD–COF after the adsorption of PFSA and PFOS, respectively (Deng et al. 2015; Wang et al. 2021). In this study, the adsorption efficiency methanol-regenerated Chi–Glu– β–CD for PFBS (Fig. 5b) decreased from 96.5 to 93.20% after the first cycle of adsorption and remained stable in the next three consecutive cycles, confirming good stability and reusability of the synthesized Chi–Glu– β–CD composite for PFBS removal.

Conclusion

In this study, an efficient and effective Chi–Glu–β–CD adsorbent was synthesized for the effective adsorptive removal of PFBS from water. The adsorption kinetics followed the PSO model and gave the rate constant value of $0.001 \pm 3\times 10^{-4}$ g mg^{-1} min^{-1}, while isotherm data fitted well to the Sips model and exhibited the high adsorption capacity of 135.70 ± 25.70 mg g^{-1} for PFBS. Different experimental conditions showed that the adsorption was highly affected by the solution pH, contact time, and initial PFBS concentration. Based on the characterization data, the adsorption mechanism confirmed the electrostatic interactions and β–CD cavity role in the PFBS adsorption. Additionally, the methanol-regenerated Chi–Glu–β–CD adsorbent showed good reusability by maintaining high adsorption capacity even after four consecutive adsorption cycles, further highlighting its potential application in water or wastewater.

Author contribution M. Verma, conceptualization, methodology, writing original draft, and editing; I. Lee, V. Kumar, S. Y. Pan, and C. Fan, review and data analysis; H. Kim, investigation and review.

Acknowledgement This work is supported by the NRF Korea under the funding BP Program (2019H1D3A1A01102657). H. Kim was supported by the Korea Environmental Industry & Technology Institute (KEITI) through the Development of Demonstration Technology for Converting Unconventional Waste Biomass to Energy, funded by the Korea Ministry of Environment (MOE) (2022003480001) and KEITI through the Post Plastic, a specialized program of the Graduate School funded by MOE. This paper is also supported by the RUDN University Strategic Academic Leadership Program.

Data availability All the relevant data are in the manuscript.

Declarations

Consent to participate and consent for publication In this study, all the authors were recruited with available informed consent. And all listed authors have agreed to submit this manuscript.

Competing interest The authors declare no competing interests.

References

Alsbaiee A, Smith BJ, Xiao L et al (2016) Rapid removal of organic micropollutants from water by a porous β-cyclodextrin polymer. Nature 529:190–194. https://doi.org/10.1038/nature16185

Badruddoza AZM, Bhattarai B, Suri RPS (2017) Environmentally friendly β-cyclodextrin-ionic liquid polyurethane-modified magnetic sorbent for the removal of PFOA, PFOS, and Cr(VI) from water. ACS Sustain Chem Eng 5:9223–9232. https://doi.org/10.1021/acssuschemeng.7b02186

Chen H, Munoz G, Duy SV et al (2020) Occurrence and distribution of per- and polyfluoroalkyl substances in Tianjin, China: the contribution of emerging and unknown analogues. Environ Sci Technol 54:14254–14264. https://doi.org/10.1021/acs.est.0c00934

Choudhary A, Dong D, Tsianou M et al (2022) Adsorption mechanism of perfluorooctanoate on cyclodextrin-based polymers: probing the synergy of electrostatic and hydrophobic interactions with molecular dynamics simulations. ACS Mater Lett 4:853–859. https://doi.org/10.1021/acsmaterialslett.2c00168

Crini G (2014) Review: a history of cyclodextrins. Chem Rev 114:10940–10975. https://doi.org/10.1021/cr500081p

Deng S, Yu Q, Huang J, Yu G (2010) Removal of perfluorooctane sulfonate from wastewater by anion exchange resins: effects of resin properties and solution chemistry. Water Res 44:5188–5195. https://doi.org/10.1016/j.watres.2010.06.038

Deng S, Nie Y, Du Z et al (2015) Enhanced adsorption of perfluorooctane sulfonate and perfluorooctanoate by bamboo-derived granular activated carbon. J Hazard Mater 282:150–157. https://doi.org/10.1016/j.jhazmat.2014.03.045

Eschauzier C, Beerendonk E, Scholte-Veenendaal P, De Voogt P (2012) Impact of treatment processes on the removal of perfluoroalkyl acids from the drinking water production chain. Environ Sci Technol 46:1708–1715. https://doi.org/10.1021/es201662b

Fan L, Luo C, Sun M et al (2013) Synthesis of magnetic β-cyclodextrin-chitosan/graphene oxide as nanoadsorbent and its application in dye adsorption and removal. Colloids Surf B Biointerfaces 103:601–607. https://doi.org/10.1016/j.colsurfb.2012.11.023

Garg S, Kumar P, Mishra V et al (2020) A review on the sources, occurrence and health risks of per-/poly-fluoroalkyl substances (PFAS) arising from the manufacture and disposal of electric and electronic products. J Water Process Eng 38:101683. https://doi.org/10.1016/j.jwpe.2020.101683

Glüge J, Scheringer M, Cousins IT et al (2020) An overview of the uses of per- and polyfluoroalkyl substances (PFAS). Environ Sci Process Impacts 22:2345–2373. https://doi.org/10.1039/d0em00291g

Houtz EF, Higgins CP, Field JA, Sedlak DL (2013) Persistence of perfluoroalkyl acid precursors in AFFF-impacted groundwater and soil. Environ Sci Technol 47:8187–8195. https://doi.org/10.1021/es4018877

Jacob P, Barzen-Hanson KA, Helbling DE (2021) Target and nontarget analysis of per- and polyfluoralkyl substances in wastewater from electronics fabrication facilities. Environ Sci Technol 55:2346–2356. https://doi.org/10.1021/acs.est.0c06690

Lenka SP, Kah M, Padhye LP (2021) A review of the occurrence, transformation, and removal of poly- and perfluoroalkyl substances (PFAS) in wastewater treatment plants. Water Res 199:117187. https://doi.org/10.1016/j.watres.2021.117187

Moody CA, Field JA (2000) Perfluorinated surfactants and the environmental implications of their use in fire-fighting foams. Environ Sci Technol 34:3864–3870. https://doi.org/10.1021/es991359u

Ochoa-Herrera V, Sierra-Alvarez R (2008) Removal of perfluorinated surfactants by sorption onto granular activated carbon, zeolite and sludge. Chemosphere 72:1588–1593. https://doi.org/10.1016/j.chemosphere.2008.04.029

OECD (2018) Toward a new comprehensive global database of per- and polyfluoroalkyl substances (PFASs): summary report on updating the OECD 2007 list of per- and polyfluoroalkyl substances (PFASs), ENV/JM/MONO:1–24

Pan Y, Zhang H, Cui Q et al (2017) First report on the occurrence and bioaccumulation of hexafluoropropylene oxide trimer acid: an emerging concern. Environ Sci Technol 51:9553–9560. https://doi.org/10.1021/acs.est.7b02259

Park M, Wu S, Lopez IJ et al (2020) Adsorption of perfluoroalkyl substances (PFAS) in groundwater by granular activated carbons: roles of hydrophobicity of PFAS and carbon characteristics. Water Res 170:115364. https://doi.org/10.1016/j.watres.2019.115364

Rae JMC, Craig L, Slone TW et al (2015) Evaluation of chronic toxicity and carcinogenicity of ammonium 2,3,3,3-tetrafluoro-2-(heptafluoropropoxy)-propanoate in Sprague-Dawley rats. Toxicol Reports 2:939–949. https://doi.org/10.1016/j.toxrep.2015.06.001

Sini K, Bourgeois D, Idouhar M et al (2018) Metal-organic framework sorbents for the removal of perfluorinated compounds in an aqueous environment. New J Chem 42:17889–17894. https://doi.org/10.1039/c8nj03312a

Son H, An B (2022) Investigation of adsorption kinetics for per- and poly-fluoroalkyl substances (PFAS) adsorption onto powder activated carbon (PAC) in the competing systems. Water Air Soil Pollut 233:1–17. https://doi.org/10.1007/s11270-022-05599-5

Trojanowicz M, Bojanowska-Czajka A, Bartosiewicz I, Kulisa K (2018) Advanced oxidation/reduction processes treatment for aqueous perfluorooctanoate (PFOA) and perfluorooctanesulfonate (PFOS) – a review of recent advances. Chem Eng J 336:170–199. https://doi.org/10.1016/j.cej.2017.10.153

Verma M, Lee I, Sharma S et al (2021) Simultaneous removal of heavy metals and ciprofloxacin micropollutants from wastewater using ethylenediaminetetraacetic acid-functionalized β-cyclodextrin-chitosan adsorbent. ACS Omega 6:34624–34634. https://doi.org/10.1021/acsomega.1c05015

Verma M, Borah R, Kumar A et al (2022a) Capturing of inorganic and organic pollutants simultaneously from complex wastewater using recyclable magnetically chitosan functionalized with EDTA adsorbent. Process Saf Environ Prot 167:56–66. https://doi.org/10.1016/j.psep.2022.09.009

Verma M, Kumar A, Lee I et al (2022b) Simultaneous capturing of mixed contaminants from wastewater using novel one-pot chitosan functionalized with EDTA and graphene oxide adsorbent. Environ Pollut 304:119130. https://doi.org/10.1016/j.envpol.2022.119130

Verma M, Lee I, Hong Y et al (2022c) Multifunctional β-cyclodextrin-EDTA-chitosan polymer adsorbent synthesis for simultaneous removal of heavy metals and organic dyes from wastewater. Environ Pollut 292:118447. https://doi.org/10.1016/j.envpol.2021.118447

Vu CT, Wu T (2020) Recent progress in adsorptive removal of per- and poly-fluoroalkyl substances (PFAS) from water/wastewater. Crit Rev Environ Sci Technol 52:90–129. https://doi.org/10.1080/10643389.2020.1816125

Wan H, Mills R, Qu K et al (2022) Rapid removal of PFOA and PFOS via modified industrial solid waste: mechanisms and influences of water matrices. Chem Eng J 433:133271. https://doi.org/10.1016/j.cej.2021.133271

Wang W, Mi X, Shi H et al (2019) Adsorption behaviour and mechanism of the PFOS substitute OBS (sodium p-perfluorous nonenoxybenzene sulfonate) on activated carbon. R Soc Open Sci 6:191069. https://doi.org/10.1098/rsos.191069

Wang W, Shao H, Zhou S et al (2021) Rapid removal of perfluoroalkanesulfonates from water by β-cyclodextrin covalent organic frameworks. ACS Appl Mater Interfaces 13:48700–48708. https://doi.org/10.1021/acsami.1c14043

Wilson LD, Pratt DY, Kozinski JA (2013) Preparation and sorption studies of β-cyclodextrin-chitosan-glutaraldehyde terpolymers. J Colloid Interface Sci 393:271–277. https://doi.org/10.1016/j.jcis.2012.10.046

Zargar V, Asghari M, Dashti A (2015) A review on chitin and chitosan polymers: structure, chemistry, solubility, derivatives, and applications. ChemBioEng Rev 2:204–226. https://doi.org/10.1002/cben.201400025

Zhao F, Sillanpää M (2020) Cross-linked chitosan and β-cyclodextrin as functional adsorbents in water treatment. In: Advanced Water Treatment. Elsevier Inc., pp 161–264

Publisher's note Springer Nature remains neutral with regard to jurisdictional claims in published maps and institutional affiliations.

Springer Nature or its licensor holds exclusive rights to this article under a publishing agreement with the author(s) or other rightsholder(s); author self-archiving of the accepted manuscript version of this article is solely governed by the terms of such publishing agreement and applicable law.